

# Preparation and Crystal Structure of New Rare Earth Bismuth Oxynitrates: $R\text{Bi}_2\text{O}_4\text{NO}_3$ ( $R$ : Y, Sm, Eu, Gd, Tb, Dy, Er, Yb)

N. Kumada,<sup>1</sup> N. Takahashi, and N. Kinomura

*Faculty of Engineering, Yamanashi University, Miyamae-cho 7, Kofu 400-8511, Japan*

and

A. W. Sleight

*Department of Chemistry, Oregon State University, Corvallis, Oregon 97331-4003*

Received November 12, 1997; in revised form April 14, 1998; accepted April 22, 1998

New rare earth bismuth oxynitrates,  $R\text{Bi}_2\text{O}_4\text{NO}_3$  ( $R$ : Y, Sm, Eu, Gd, Tb, Dy, Er, Yb) were prepared with low temperature hydrothermal reactions using  $\text{NaBiO}_3 \cdot n\text{H}_2\text{O}$  and  $R(\text{NO}_3)_3 \cdot n\text{H}_2\text{O}$  as starting materials. These rare earth bismuth oxynitrates crystallized in the tetragonal system with space group  $P4mm$  and  $Z = 1$ . The lattice parameters depend on the ionic radius of rare earth atoms and range from  $a = 3.8470(1)$  and  $c = 10.1762(7)$  Å for  $R = \text{Yb}$  to  $a = 3.9038(1)$  and  $c = 10.2370(5)$  Å for  $R = \text{Sm}$ . The crystal structure for  $R = \text{Y}$  was refined using neutron powder diffraction data, with the final  $R$  factors being  $R_{\text{wp}} = 4.35$ ,  $R_{\text{p}} = 3.29$ ,  $R_1 = 5.39$ , and  $R_F = 4.40\%$ .  $R\text{Bi}_2\text{O}_4\text{NO}_3$  is isostructural with  $R'_x\text{Bi}_{3-x}\text{O}_4\text{X}$  ( $R'$ : La, Ce, Nd, Eu, Gd;  $X$ : Cl, Br, Se) having a layered structure based on  $(R\text{Bi}_2\text{O}_4)^+$  and  $(\text{NO}_3)^-$  layers. There are three kinds of metal atom positions, all coordinated by eight oxygens; one is occupied by Y atoms and the other two are filled with Bi atoms. On heating above  $500^\circ\text{C}$  this compound decomposes to the solid solution  $(R,\text{Bi})_2\text{O}_3$  accompanied by the evolution of NO and  $\text{O}_2$ . © 1998 Academic Press

## INTRODUCTION

We have prepared several new bismuth oxides by low temperature hydrothermal reactions using hydrate sodium bismuth oxide,  $\text{NaBiO}_3 \cdot n\text{H}_2\text{O}$ , as one of the starting materials (1–7). During these studies a new lanthanum bismuth oxyhydroxide,  $(\text{La},\text{Bi})\text{OOH}$  with a  $\text{BiOCl}$ -type related structure was prepared by using lanthanum nitrate as one of the starting materials (2). For other rare earth nitrates, the new rare earth bismuth oxynitrates  $R\text{Bi}_2\text{O}_4\text{NO}_3$  ( $R$ : Y, Sm,

Eu, Gd, Tb, Dy, Er, Yb) were prepared; their crystal structures are isostructural with those of  $R'_x\text{Bi}_{3-x}\text{O}_4\text{X}$  ( $R'$ : La, Ce, Nd, Eu, Gd;  $X$ : Cl, Br, Se).

In the  $\text{Bi}_2\text{O}_3\text{--NO}_3^-$  system, there are two known compounds,  $\text{BiONO}_3$  (8) and  $\text{Bi}_5\text{O}_7\text{NO}_3$  (9). The crystal structure of  $\text{BiONO}_3$  has not yet been determined, and  $\text{Bi}_5\text{O}_7\text{NO}_3$  prepared by thermal decomposition of  $\text{Bi}(\text{NO}_3)_3 \cdot 5\text{H}_2\text{O}$  is isostructural with  $\text{Bi}_5\text{O}_7\text{I}$ . Recently, a new yttrium oxynitrate,  $\text{YONO}_3$ , was prepared by thermal decomposition of  $\text{Y}(\text{NO}_3)_3 \cdot 5\text{H}_2\text{O}$ , and its crystal structure was reported to be similar to that of  $\text{BiOCl}$  (10). The crystal structure of  $R\text{Bi}_2\text{O}_4\text{NO}_3$  is based on  $(R\text{Bi}_2\text{O}_4)^+$  layers and is distinct from the  $\text{BiOCl}$  type structure, which has  $(\text{Bi}_2\text{O}_2)^{2+}$  layers. These two structures will be further compared in this paper.

## EXPERIMENTAL

### 1. Sample Preparation and Characterization

Powder of  $\text{NaBiO}_3 \cdot n\text{H}_2\text{O}$  (Nacalai Tesque Inc.) was placed in a teflon-lined autoclave (70 ml) with the rare earth nitrate  $R(\text{NO}_3)_3 \cdot n\text{H}_2\text{O}$  ( $R$ : Y, Ce, Nd, Sm, Eu, Gd, Tb, Dy, Er, Yb) and  $\text{H}_2\text{O}$  (30 ml), which was heated at  $120\text{--}200^\circ\text{C}$  for 4 days. The molar ratio of  $\text{NaBiO}_3 \cdot n\text{H}_2\text{O}$  and rare earth nitrate was varied from 0.25 to 8. The solid products were separated by centrifuging, washed with distilled water, and dried at  $50^\circ\text{C}$ . The products were identified by X-ray powder diffraction using Ni-filtered  $\text{CuK}\alpha$  radiation. The products were completely dissolved in a concentrated HCl and  $\text{HNO}_3$  mixture, and the amounts of sodium, rare earth, and bismuth in the solution were analyzed by atomic absorption spectroscopy or inductively coupled plasma spectroscopy. The valence of bismuth was determined by idometric titration. The thermal stability was investigated by TG–DTA

<sup>1</sup>To whom correspondence should be addressed. E-mail: kumada@mail.yamanashi.ac.jp.

with a heating rate of  $10^\circ/\text{min}$ . The species evolved during TG–DTA measurement in a stream of He was analyzed by mass spectrometry.

## 2. Crystal Structure Refinement

For the structural refinement by neutron diffraction, intensity data were collected at 295 K on a high-resolution powder diffractometer at the Brookhaven National Laboratory. The data were recorded at intervals of  $0.05^\circ$  in  $2\theta$  from  $10.00$  to  $156.75^\circ$  using a wavelength of  $1.8857\text{ \AA}$ . Rietveld structural analysis was performed using the program RIETAN (11).

## RESULTS AND DISCUSSION

### 1. Preparation

Single-phase  $\text{RBi}_2\text{O}_4\text{NO}_3$  phases were obtained by reactions at  $140\text{--}200^\circ\text{C}$  for 2 days using the molar ratios of  $\text{R}/\text{Bi} = 0.5\text{--}8$  for  $\text{R} = \text{Y}, \text{Sm}, \text{Eu}, \text{Gd}, \text{Tb}, \text{Dy}, \text{Er}, \text{Yb}$ . The X-ray powder patterns were indexed in the tetragonal system with  $a \sim 3.8\text{ \AA}$  and  $c \sim 10.2\text{ \AA}$  as summarized in Table 1. The lattice parameters depend on the ionic radius of rare earth as shown in Fig. 1. From the chemical analysis, the molar ratio of  $\text{Bi}/\text{R}$  in the products was found to be two, and no sodium was detected. The mean valence of bismuth was determined to be three. Figure 2 shows the IR spectrum for the product of  $\text{R} = \text{Y}$ , and the strong absorption at  $1380\text{ cm}^{-1}$  was assigned to the  $(\text{NO}_3)^-$  group. The chemical analysis for  $\text{R} = \text{Y}$  is summarized in Table 2. The molar ratio of  $\text{Bi}/\text{Y}$  was independent of the preparative condition. As mentioned later, the weight loss was caused by the release of the nitrate group. Therefore, the chemical composition may be represented as  $\text{RBi}_2\text{O}_4\text{NO}_3$ .

The X-ray powder pattern of the product for  $\text{R} = \text{Nd}$  indicated that this product is isostructural with the lanthanum bismuth oxyhydroxide,  $\text{La}_{0.26}\text{Bi}_{0.74}\text{OOH}$  (2). The X-ray powder pattern of the product for  $\text{R} = \text{Pr}$  was similar to that of  $\text{RBi}_2\text{O}_4\text{NO}_3$ , however, several weak unindexed

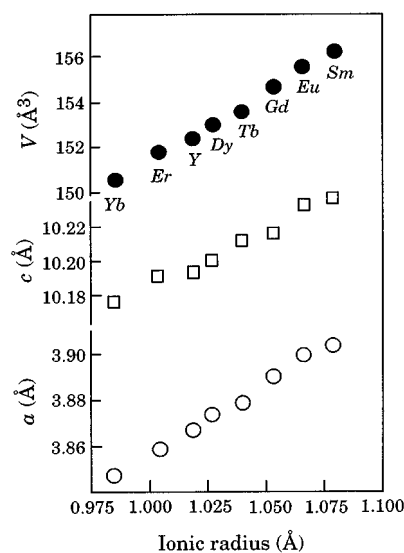


FIG. 1. Lattice parameters and unit cell volumes plotted against ionic radius of R ions for  $\text{RBi}_2\text{O}_4\text{NO}_3$ .

peaks were observed. The products for  $\text{R} = \text{Ce}$  were not well crystallized.

### 2. Thermal Behavior

Figure 3 shows the TG–DTA curves and gas evolution during the TG–DTA measurement for  $\text{YBi}_2\text{O}_4\text{NO}_3$ . The one-step weight loss is observed above  $400^\circ\text{C}$  and is caused by the release of  $\text{NO}$  and  $\text{O}_2$ . The observed weight loss (8.63 wt%) agrees well with the value (8.53 wt%) calculated on the assumption that the  $\text{NO}_3$  group is released from  $\text{YBi}_2\text{O}_4\text{NO}_3$ . The X-ray powder pattern of the sample heated to  $800^\circ\text{C}$  corresponds to that of the cubic  $(\text{Y,Bi})_2\text{O}_3$  (12).

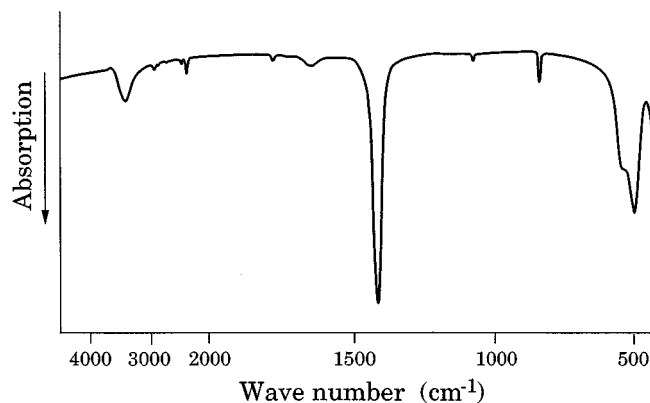


FIG. 2. Infrared spectrum for  $\text{YBi}_2\text{O}_4\text{NO}_3$ .

TABLE 1  
The Lattice Parameters and Unit Cell Volumes for  $\text{RBi}_2\text{O}_4\text{NO}_3$

R	$a$ (Å)	$c$ (Å)	$V$ (Å <sup>3</sup> )
Sm	3.9038(1)	10.2370(5)	156.19
Eu	3.8996(1)	10.2331(7)	155.61
Gd	3.8905(1)	10.2163(6)	154.63
Tb	3.8790(2)	10.212(1)	153.66
Dy	3.8740(1)	10.2003(7)	153.08
Y	3.8671(1)	10.1930(3)	152.43
Er	3.8587(2)	10.1914(7)	151.75
Yb	3.8470(1)	10.1762(7)	150.60

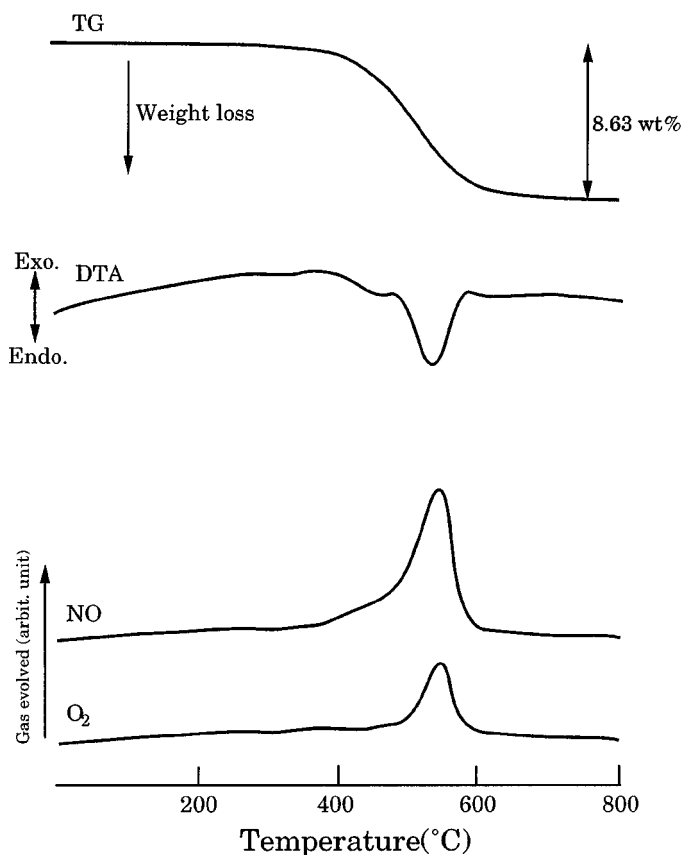


FIG. 3. TG-DTA curves and gas evolution during TG-DTA measurement for  $\text{YBi}_2\text{O}_4\text{NO}_3$ .

### 3. Crystal Structure

The  $\text{RBi}_2\text{O}_4\text{NO}_3$  composition may be considered a member of the  $\text{M}_3\text{O}_4\text{X}$  ( $M$ , metal;  $X$ , halogen) family in which  $\text{R}'_x\text{Bi}_{3-x}\text{O}_4\text{X}$  ( $\text{R}'$ : La, Ce, Nd, Eu, Gd;  $X$ : Cl, Br, Se) and

TABLE 2  
Chemical Analysis  $(\text{Y, Bi})_3\text{O}_4\text{NO}_3$

	$\text{Y}_2\text{O}_3$	$\text{Bi}_2\text{O}_3$	Weight loss	Total
Calculated (wt%)	17.84	73.63	8.53	100.0
Observed (wt%)	17.00	74.28	8.63	99.91

$\text{Bi}_3\text{O}_4\text{X}$  ( $X$ : Cl, Br) are known (13). Their crystal structures are built up from a fluorite-type  $(\text{M}_3\text{O}_4)^+$  layer and a single halogen layer. The former has the tetragonal cell with  $a \sim 3.9 \text{ \AA}$  and  $c \sim 8.9 \text{ \AA}$  and the latter is distorted to monoclinic. The similarity of cell dimensions of  $\text{RBi}_2\text{O}_4\text{NO}_3$  and  $\text{R}'_x\text{Bi}_{3-x}\text{O}_4\text{X}$  suggests that the crystal structure of  $\text{RBi}_2\text{O}_4\text{NO}_3$  can be derived by replacing the halogen atom in  $\text{R}'_x\text{Bi}_{3-x}\text{O}_4\text{X}$  with the  $(\text{NO}_3)^-$  group.

The neutron diffraction pattern for  $\text{YBi}_2\text{O}_4\text{NO}_3$  was indexed with the same tetragonal cell used for the X-ray powder pattern, and no extra diffraction peaks due to a superstructure were observed. No systematic absences for reflections were observed in the X-ray and neutron powder diffraction patterns; therefore, eight space groups with tetragonal symmetry are possible. Of these space groups  $P4$  (No. 75) and  $P4mm$  (No. 99) allow a structural model having a set of  $(\text{M}_3\text{O}_4)^+$  layers and  $(\text{NO}_3)^-$  groups as in the crystal structure of  $\text{R}'_x\text{Bi}_{3-x}\text{O}_4\text{X}$ . The Rietveld structural refinement using the neutron diffraction data led to reasonable  $R$  factors;  $R_{\text{WP}} = 4.47$ ,  $R_{\text{P}} = 3.40$ ,  $R_{\text{I}} = 5.67$ , and  $R_{\text{F}} = 4.68\%$  for  $P4$  and  $R_{\text{WP}} = 4.35$ ,  $R_{\text{P}} = 3.29$ ,  $R_{\text{I}} = 5.39$ , and  $R_{\text{F}} = 4.40\%$  for  $P4mm$ . However, in the case of  $P4$  the refined positional parameters of one oxygen in the  $(\text{NO}_3)^-$  group, in which the starting positions of oxygen atoms were estimated from N-O distance, had unreasonable values. Therefore, the structural model using the space group  $P4mm$

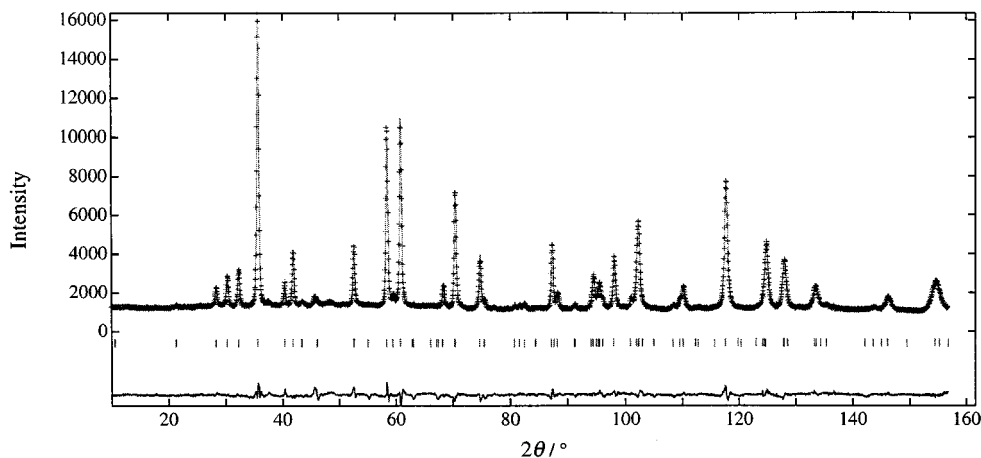


FIG. 4. Observed (dots), calculated (solid line), and difference (bottom) neutron diffraction profiles for  $\text{YBi}_2\text{O}_4\text{NO}_3$ .

**TABLE 3**  
Crystal Data and Intensity Collection for  $\text{YBi}_2\text{O}_4\text{NO}_3$

Color	Yellow
Crystal system	Tetragonal
Space group	$P4mm$ (No. 99)
Z	1
Lattice parameters	$a = 3.8671(1)$ , $c = 10.1930(3)$ Å
Volume	$152.43$ Å <sup>3</sup>
Formula weight	632.83
Calculated density	$6.89$ g/cm <sup>3</sup>
Wavelength	$\lambda = 1.8857$ Å
Temperature	$23^\circ\text{C}$
$2\theta$ scan range	$10.00$ – $156.75^\circ$
$R_{\text{WP}}$	4.35%
$R_{\text{P}}$	3.29%
$R_{\text{I}}$	5.39%
$R_{\text{F}}$	4.40%

was adopted. Since the twofold axis of the  $(\text{NO}_3)^-$  is parallel to the  $c$  axis (fourfold axis), two oxygen atoms of the  $(\text{NO}_3)^-$  group in the  $ab$  plane must be statistically distributed in the  $4e$  site. The occupancy of the oxygen atom at the  $4e$  site refined to 0.48(6). Thus, the orientation of the  $(\text{NO}_3)^-$  groups is an average in which the adjacent  $(\text{NO}_3)^-$  groups stand at right angles to each other, and in this case the shortest O–O distance has a reasonable value of  $2.98(2)$  Å as mentioned later. A similar average structure for  $(\text{NO}_3)^-$  groups is also observed in  $\text{YONO}_3$  (10).

Figure 4 shows observed and calculated neutron diffraction patterns. The crystallographic data and atomic parameters are summarized in Tables 3 and 4, respectively. Selected interatomic distances are listed in Table 5. As shown in Fig. 5, the crystal structure of  $\text{YBi}_2\text{O}_4\text{NO}_3$  is built up by alternate stacking of  $(\text{M}_3\text{O}_4)^+$  layers and  $(\text{NO}_3)^-$  groups along the  $c$  axis. There are three kinds of metal atom sites in the  $(\text{M}_3\text{O}_4)^+$  layer. Yttrium atoms at the center of the layer are coordinated by eight oxygen atoms to form a cube with interatomic distances of  $2.38(3)$  and  $2.40(3)$  Å. Two bismuth atoms have similar environments with eight

**TABLE 5**  
Selected Interatomic Distances (Å) for  $\text{YBi}_2\text{O}_4\text{NO}_3$

Y–O(1)	$2.38(3) \times 4$	Bi(1)–O(2)	$2.19(2) \times 4$
O(2)	$2.40(3) \times 4$	O(3)	$3.03(2) \times 4$
mean	2.39	mean	2.61
O(1)–O(1)	$2.734 \times 4$	O(2)–O(2)	2.734
O(2)–O(2)	$2.734 \times 4$	O(3)–O(3)	3.867
Bi(2)–O(1)	$2.27(3) \times 4$	N–O(3)	1.30(6)
O(4)	$2.92(4) \times 4$	O(4)	$1.23(4) \times 2$
mean	2.60	mean	1.25
O(1)–O(1)	$2.734 \times 4$	O(3)–O(4)	$2.15(6) \times 2$
O(4)–O(4)	$2.98(2) \times 4$	O(4)–O(4)	2.19(7)

oxygen atoms to form square antiprism. The square antiprism around the Bi(1) atom is formed by O(2) from the  $(\text{M}_3\text{O}_4)^+$  layer and O(3) from the  $(\text{NO}_3)^-$  group, and the interatomic distances are  $2.19(2)$  and  $3.03(2)$  Å, respectively. The square antiprism around the Bi(2) atom formed by O(1) and O(4) atoms is somewhat distorted, as shown in Fig. 6. The Bi(2)–O(1) and O(4) distances are  $2.27(3)$  and  $2.92(2)$  Å, and the O(4)–O(4) distance in this polyhedron corresponds to the shortest O–O distance between the adjacent  $(\text{NO}_3)^-$  groups. In the  $(\text{NO}_3)^-$  group, the N–O distances are  $1.23(4)$  and  $1.30(6)$  Å, agreeing well with the N–O distances of  $1.23(3)$ – $1.28(2)$  in  $\text{Bi}(\text{NO}_3)_3 \cdot 5\text{H}_2\text{O}$ , which were determined by using single-crystal X-ray diffraction data (14).

The  $R'_x\text{Bi}_{3-x}\text{O}_4\text{X}$  solid solution has a wide range ( $1 \leq x \leq 2$ ) in contrast to  $\text{YBi}_2\text{O}_4\text{NO}_3$ . In the case of  $\text{Nd}_{0.5}\text{Bi}_{2.5}\text{O}_4\text{Cl}$  ( $x = 0.5$ ), neodymium and bismuth atoms are statistically distributed at the site with the eightfold coordination. The refinement of the disordered model for  $\text{YBi}_2\text{O}_4\text{NO}_3$  led to  $R_{\text{WP}} = 4.20$ ,  $R_{\text{P}} = 3.18$ ,  $R_{\text{I}} = 4.16$ , and  $R_{\text{F}} = 3.03\%$ , being somewhat better than those for the ordered model. However, the mean metal–oxygen distance

**TABLE 4**  
Positional and Thermal Parameters (Å) for  $\text{YBi}_2\text{O}_4\text{NO}_3$

Atom	Site	Occupancy	$x$	$y$	$z$	$B_{\text{iso}}$
Y	1a	1	0	0	0	0.4(2)
Bi(1)	1b	1	0.5	0.5	0.240(5)	0.9(7)
Bi(2)	1b	1	0.5	0.5	0.748(5)	0.7(9)
O(1)	2c	1	0.5	0	0.864(5)	0.8(7)
O(2)	2c	1	0.5	0	0.139(6)	0.5(6)
O(3)	1a	1	0	0	0.369(6)	2.8(8)
O(4)	4e	0.48(6)	0.284(9)	0	0.550(6)	3(1)
N	1a	1	0	0	0.497(6)	0.3(4)

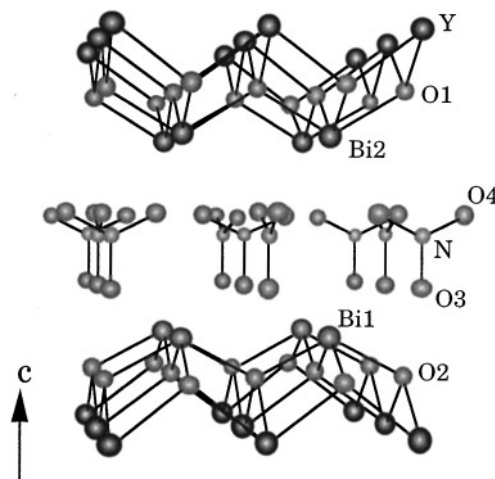


**FIG. 5.** Crystal structure of  $\text{YBi}_2\text{O}_4\text{NO}_3$ .

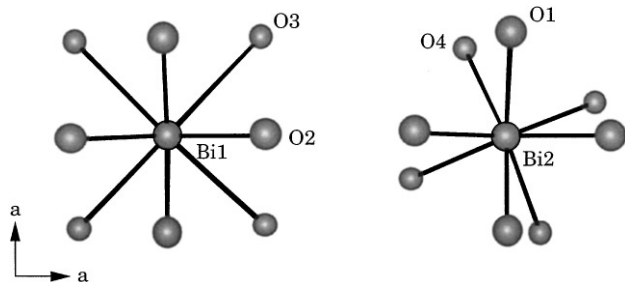


FIG. 6. Coordination environments around Bi(1) and Bi(2) atoms.

(2.39 Å) for one of three metal sites was shorter than those (2.60 and 2.63 Å) for the other sites as observed in the ordered model. By taking into account the difference between ionic radii of yttrium and bismuth and the chemical composition of Bi/Y = 2, the ordered model is considered to be reasonable.

The Sillen structures are based on  $(\text{Bi}_2\text{O}_2)^{2+}$  layers and are classified by the way of stacking  $(\text{Bi}_2\text{O}_2)^{2+}$  layers ( $M$ ) and halide layers ( $X$ ); for example, the  $X1$  structure can be described as the stacking of layers in sequence  $-M-X-M-$  as found in  $\text{CaBiO}_2\text{Cl}$ , and the  $X2$  has the  $-M-X-X-M-$  sequence as in  $\text{BiOCl}$  (15). A bismuth oxycarbonate,  $\text{Bi}_2\text{O}_2\text{CO}_3$ , also has the Sillen structure and belongs to the  $X1$  structure (16). There are many bismuth oxyhalides distinct from the Sillen structures, such as,  $\text{BiM}_3\text{O}_3\text{Cl}_3$  ( $M = \text{Ca}, \text{Sr}$ ) (17) and  $\text{Bi}_3\text{PbWO}_8\text{Cl}$  (18). The latter is one of bipox structure series compounds with a mixed Aurivillius–Sillen structure. Also,  $R'_x\text{Bi}_{3-x}\text{O}_4\text{X}$  and  $\text{RBi}_2\text{O}_4\text{NO}_3$  do not have the Sillen structure, however, the  $(\text{M}_3\text{O}_4)^+$  layer in  $R'_x\text{Bi}_{3-x}\text{O}_4\text{X}$  and  $\text{RBi}_2\text{O}_4\text{NO}_3$  can be derived by insertion of  $(\text{MO})^-$  layers into the  $(\text{Bi}_2\text{O}_2)^{2+}$  layers of the Sillen structure. In this respect these compounds may be regarded as a derivative of the Sillen structure.

## CONCLUSION

New rare earth bismuth oxynitrates  $\text{RBi}_2\text{O}_4\text{NO}_3$  ( $R$ : Y, Sm, Eu, Gd, Tb, Dy, Er, Yb) were prepared with low temperature hydrothermal reactions. The crystal structure of  $\text{RBi}_2\text{O}_4\text{NO}_3$  is based on  $(\text{RBi}_2\text{O}_4)^+$  and  $(\text{NO}_3)^-$  layers and is derived by replacing the halogen atoms in  $R'_x\text{Bi}_{3-x}\text{O}_4\text{X}$  with  $(\text{NO}_3)^-$  groups.  $\text{RBi}_2\text{O}_4\text{NO}_3$  phases are the first examples of a  $R'_x\text{Bi}_{3-x}\text{O}_4\text{X}$ -type structure where  $X$  is a  $(\text{NO}_3)^-$  group.

## REFERENCES

1. N. Kumada, M. Hosoda, and N. Kinomura, *J. Solid State Chem.* **106**, 476 (1993).
2. N. Kumada, N. Kinomura, S. Kodialam, and A. W. Sleight, *Mater. Res. Bull.* **26**, 497 (1994).
3. S. Kodialam, N. Kumada, R. Mackey, and A. W. Sleight, *Eur. J. Solid State Inorg. Chem.* **31**, 739 (1994).
4. N. Kinomura and N. Kumada, *Mater. Res. Bull.* **30**, 129 (1995).
5. N. Kumada, N. Kinomura, P. M. Woodward, and A. W. Sleight, *J. Solid State Chem.* **116**, 281 (1995).
6. N. Kumada, N. Kinomura, N. Takahashi, and A. W. Sleight, *J. Solid State Chem.* **126**, 121 (1996).
7. N. Kumada, N. Kinomura, N. Takahashi, and A. W. Sleight, *Mater. Res. Bull.* **32**, 1003 (1997).
8. Gmelin-Institute, "Gmelin Handbuch der anorganische chemie, Bismuth," System-Number 19, p. 656. Springer-Verlag, Berlin/Heidelberg/New York, 1964.
9. H. Kodama, *J. Solid State Chem.* **112**, 27 (1994).
10. D. Pelloquin, M. Louer, and D. Louer, *J. Solid State Chem.* **112**, 182 (1994).
11. F. Izumi, *Kobutsugaku Zasshi* **17**, 37 (1985).
12. T. Takahashi and H. Iwahara, *Mater. Res. Bull.* **13**, 1447 (1978).
13. B. Aurivillius, *Chemica Scripta* **24**, 125 (1984).
14. F. Lazarini, *Acta Crystallogr. C* **41**, 1144 (1985).
15. L. G. Sillen, *Z. Anorg. Allg. Chem.* **248**, 121 (1941).
16. C. Greaves and S. K. Blower, *Mater. Res. Bull.* **23**, 1001 (1988).
17. J. Huang and A. W. Sleight, *J. Solid State Chem.* **96**, 154 (1992).
18. J. F. Ackerman, *J. Solid State Chem.* **62**, 92 (1986).